

Reconstruction of the Near-Surface Model in Complex Seismogeological Conditions of Eastern Siberia Utilizing Full Waveform Inversion with Varying Topography

Kirill Gadylshin[1(✉)], Vladimir Tcheverda[1], and Danila Tverdokhlebov[2]

[1] Institute of Petroleum Geology and Geophysics SB RAS, 3 Koptug ave., Novosibirsk 630090, Russia
GadylshinKG@ipgg.sbras.ru

[2] LLC RN-Exploration, 8 Mozhaisky Val st., Moscow 121151, Russia

Abstract. Seismic surveys in the vast territory of Eastern Siberia are carried out in seismic and geological conditions of varying complexity. Obtaining a high-quality dynamic seismic image for the area of work is a priority task in the conditions of contrasting heterogeneities of the near-surface. For this, it is necessary to restore an effective depth-velocity model that provides compensation for velocity anomalies and calculates static corrections. However, for the most complex near-surface structure, for example, the presence of trap intrusions and tuffaceous formations, the information content of the velocity models of the near-surface area obtained on the basis of tomographic refinement turns out to be insufficient, and a search for another solution is required. The paper considers an approach based on the full waveform inversion (FWI). As the authors showed earlier, the use of multiples associated with the free surface reduces the resolution of this approach but increases the stability of the solution in the presence of uncorrelated noise. Therefore, at the first stage of FWI, the entire wavefield is used, including free surface-related multiples. The data after the suppression of multiples is then used. The obtained results demonstrate the ability of the FWI to restore complex geological structures of the near-surface area, even in the presence of high-velocity anomalies (trap intrusions).

Keywords: Near-surface · Full waveform inversion · Free surface topography

1 Introduction

This work, to some extent, acts as a development of our previous studies devoted to the consideration of full-waveform inversion for the reconstruction of deep

Supported by RSF grant 21-71-20002.

© Springer Nature Switzerland AG 2021
O. Gervasi et al. (Eds.): ICCSA 2021, LNCS 12949, pp. 504–518, 2021.
https://doi.org/10.1007/978-3-030-86653-2_37

horizons (see [4,6]). Previously, we focused our attention on geological media with an effortless top of the section, typical for marine seismic observations. However, when conducting seismic observations on land, the assumption about the simplicity of the upper part of the section's structure is no longer valid, especially for Eastern Siberia. Here we are presenting our approach to the reconstruction of geological media with a complicated upper section. Really, the correct near-surface contribution is necessary when determining the structural features of the reconstruction of the geological media (shape and the location of the interfaces) and searching for its seismic parameters, like wave propagation velocities (inverse dynamic problem). Distortion of results obtained using an imprecise model of near-surface will introduce significant errors both in the depth and the shape of the target horizons, not to mention the correct restoration of their lateral variability [3].

In this regard, near-surface structure reconstruction is one of the most demanded among a wide range of seismic studies [1,2,8]. It can be argued that it is a fairly developed seismic exploration area that uses a diverse set of methods and techniques. We list only the main approaches to solve it, which we know:

- solution of the inverse kinematic problem with the subsequent introduction of the obtained static corrections. The solution here is built for near-surface layers in order to calculate the required time shifts to the original seismograms, which avoids artificial curvature of the target horizons and ensures the correct focusing of wave seismic images [9];
- application of seismic tomography methods on refracted rays for the reconstruction of the velocity structure of the near-surface and its subsequent use in calculating static corrections and constructing wave seismic images of target horizons [9,10];
- determination of the velocity structure of the near-surface using surface waves [11,12];
- full-waveform inversion methods oriented on the near-surface area [13,14].

To better understand the possibility of reconstructing the near-surface area's velocity model, it is necessary to carry out special work on seismic geological modelling. The work authors built a detailed seismogeological model based on all available geological and geophysical information for performing finite-difference modelling. As a result of modelling, high-quality synthetic data were obtained that are close to real seismic materials, which were subsequently used for full-waveform inversion.

The thickness of the sedimentary cover in the study area reaches 1600–2000 m. The upper and basal parts of the section are represented by terrigenous rocks, in the middle and lower parts - by alternating halogen and carbonate layers. The section is complicated by several levels of intrusion of magmatic intrusions. Trap intrusions and tuffaceous formations complicate the near-surface. The target horizons (terrigenous and carbonate strata) lie at the base of the section. The reservoir thickness is 10–15 m. The section's complex structure is determined by seismic and geological heterogeneities, leading to the formation of sharp and significant vertical and lateral variations in the elastic characteristics

of the medium. The sizes of submerged velocity anomalies, such as intrusions, can vary from the first tens to thousands of meters, and the depth of occurrence may reach $\frac{3}{4}$ or more of the depth of the sedimentary cover. Differences in the terrain up to 200–400 m with sharp slopes of ravines and indented river valleys, exposing various types of rocks on the surface, lead not only to the complexity of restoration and taking into account the velocity characteristics of the section but also to significant variations in amplitude-frequency characteristics of the seismic signal over the area of work.

All inhomogeneities in the near-surface lead to the formation of a huge number of interference waves, which nature is not always possible to reliably identify, and which reduce the efficiency or make it useless and even impossible to use "standard" seismic processing procedures, including reconstruction of the near-surface velocity model. To improve the quality and reliability of the processing and interpretation results, it becomes necessary to carry out an in-depth analysis of the influence of changes in seismic-geological conditions on the characteristics of the seismic record and its possibility recovering a high-quality dynamic image. To assess the feasibility of algorithms and methods for reconstructing the near-surface, one needs to use synthetic seismic data modelled based on a detailed thin-layered model containing characteristic seismogeological features as close as possible to the real studied section. Based on the testing results on synthesized data based on a well-known model, one should adapt the algorithms to work on real seismic data.

2 Seismogeological Model Building

Seismic surveys in the vast territory of Eastern Siberia are carried out in seismic and geological conditions of varying complexity. The selected area to build a seismogeological model is Irkutsk region, Russia (Fig. 1). It contains anomalous and target geological objects. The original thick-layered model was built based on information about the topography and stratigraphic information from well data (Fig. 2). For detailing the near-surface model, anomalies were specified based on information about tuffs and traps' location according to a geological map. The geometry of intrusions, trap and tuff formations, as well as supply channels for the first 500m, was set according to the interpretation of non-seismic methods - electrical prospecting and gravity magnetic prospecting based on conceptual forms of volcano structures of diamondiferous regions in adjacent territories, studied in detail by drilling wells [7]. Velocity characteristics were included in the model according to well logging data. Schematically, the evolution of model building is shown in Fig. 2.

3 Method

The inverse dynamic problem is considered as a solution of a nonlinear operator equation

$$F(m) = d, \tag{1}$$

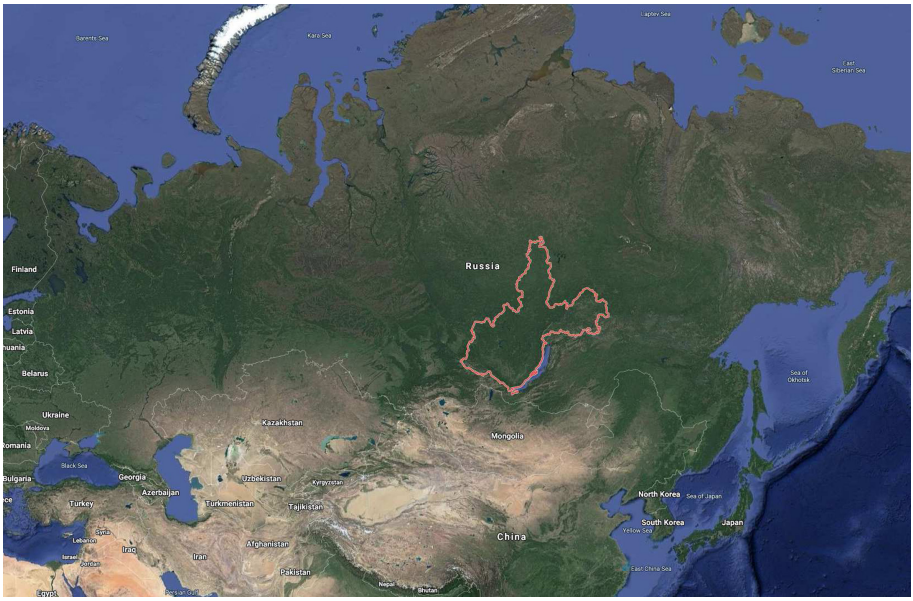

Fig. 1. The location map of the studied area. The borders of the Irkutsk region are marked in red. (Color figure online)

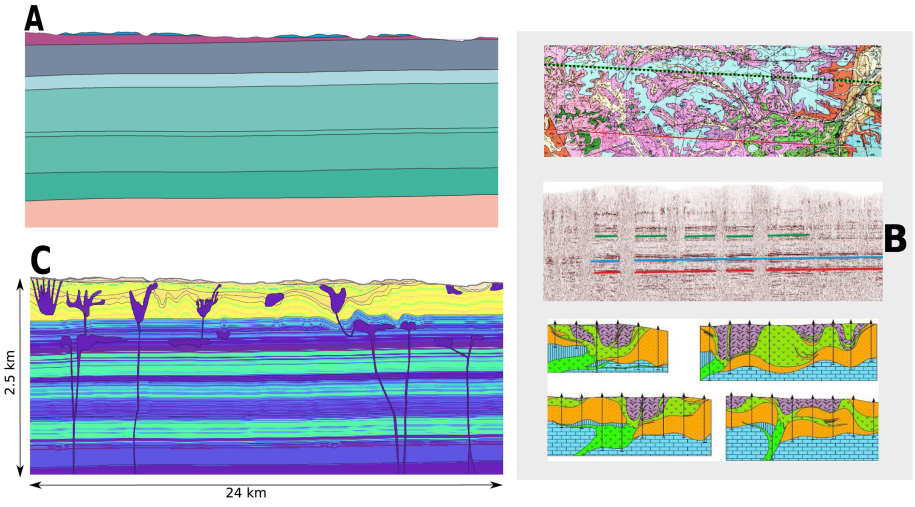

Fig. 2. The evolution of the depth model building for pressure velocities. The original thick-layered model constructed using topography and well log data (a), detailing of the model using geological maps and well information (b) and the final P-velocity model (c).

where $F : M \to D$ is a nonlinear forward operator which maps model space M into data space D. To simplify mathematical calculations, we deal with the scalar wave equation in the time domain, that is, the Helmholtz equation:

$$\triangle u(x,z) + \frac{\omega^2}{c^2(x,z)} u = f(\omega)\delta(x - x_s)\delta(z - z_s), \tag{2}$$

with absorbing boundary conditions on the base of perfectly matched layers (PML). Here (x_s, z_s) determine the coordinates of the source with the pulse shape $f(\omega)$. Calculation of the solution of the formulated problem at the location of the receivers determines the forward modelling operator F. We solve this equation using the fourth order finite difference scheme, which leads to a sparse system of linear algebraic equations (SLAE). This SLAE is solved using direct LU-based method.

The common full-waveform inversion formulation is to find the minimum point of the misfit functional, characterizing the mean square deviation of the registered data from the calculated for the current speed model:

$$m^* = argmin_{m \in M}(\|F(m) - d\|_D^2), \tag{3}$$

where $m(x,z) = c^{-2}(x,z)$ - squared slowness.

Typically, the local optimization techniques, such as conjugate gradient method, are applied to minimize the misfit function:

$$m_{k+1} = m_k + \mu_k S_k,\ S_0 = \nabla_0, \tag{4}$$

$$S_k = -\nabla_k - \frac{< \nabla_k, \nabla_k - \nabla_{k-1} >_M}{< \nabla_k, \nabla_{k-1} >_M} S_{k-1}, \tag{5}$$

where m_k – model on k-th iteration. The gradient ∇_k is calculated as follows:

$$\nabla_k = \Re\{DF^* \delta d_k\} \tag{6}$$

here $\delta d_k = F(m_k) - d$ is data residual on current iteration, DF – first derivative of forward map calculated at point m_k.

For efficient gradient calculation, we use a master/slave communication Message Passing Interface (MPI) scheme (see Fig. 3). Considering that we use Nf time-frequencies for FWI, the algorithm requires one master MPI-process and Nf slave processes. Slave MPI-process with index i calculate partial gradient for a particular time-frequency f_i and associated with the corresponding Helmholtz equation (Fig. 3). Within a single slave MPI-process, the Helmholtz equation solver is parallelized via OpenMP. On the next step, the master process gathers all partial gradients, performs the model update and send the updated model back to the slave processes. This process repeats iteratively until the convergence conditions are not satisfied.

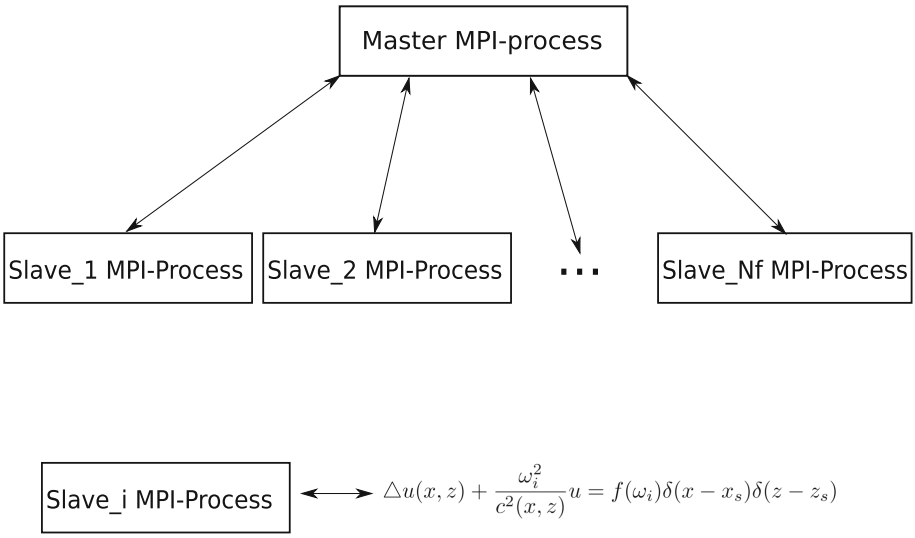

Fig. 3. The schematic master/slave communication of the FWI algorithm. Each slave MPI-process is related to the Helmholtz equation for a fixed time frequency.

4 Numerical Experiments

4.1 Model and Acquisition Geometry

We used a realistic P-velocity profile in our numerical experiments, which building process described in Sect. 2. For FWI, we choose a part of the model, designated by a red rectangle in Fig. 4. The horizontal size of the model is 24 km, while the depth reaches 2.8 km. The main difficulty in reconstructing the near-surface area caused by the presence of trap intrusions, the velocity of propagation of P-waves in which reaches 6500 m/s, thus the velocity difference when crossing the intrusion boundary reaches 4500 m/s, which significantly complicates the use of standard approaches to recover the depth velocity model. The presence of varying topography also complicates the velocity model building. It is necessary to perform full-waveform modelling on a fine mesh to mitigate numerical dispersion caused by staircase topography approximation on a rectangular grid. An example of a synthetic seismogram calculated in acoustic mode, taking into account the multiples caused by the presence of a free surface, is shown in Fig. 5. The acquisition system has 241 seismic sources and 961 receivers located at the free surface with a lateral spacing of 100 m and 25 m. The maximum source-receiver offset is 5 km. The source impulse is a Ricker wavelet with a dominant frequency 30 Hz. As an initial guess for FWI, we used a vertically heterogeneous model (see Fig. 6), which was built using the well information (x = 20 km in the true model) by Gaussian smoothing and adding a free surface topography. Thus, the starting depth velocity model contains no information about the presence of high-velocity near-surface anomalies.

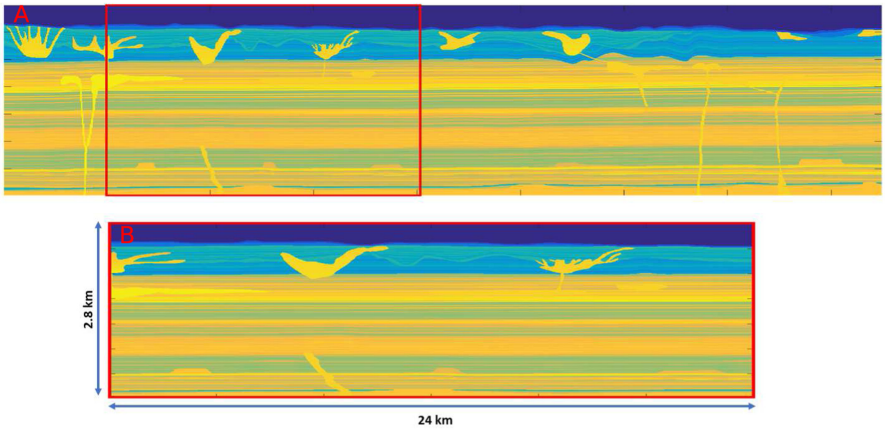

Fig. 4. The full P-velocity profile obtained after seismogeological model building (a) and the area used for performing FWI experiments (b).

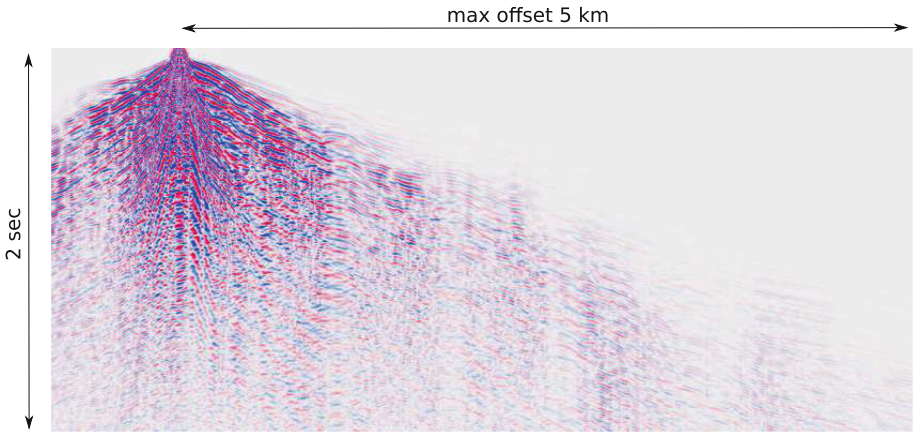

Fig. 5. The example of observed seismogram used for near-surface FWI.

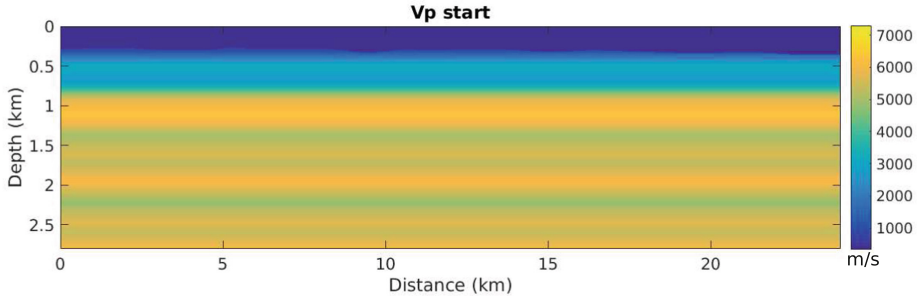

Fig. 6. The starting depth velocity model for near-surface FWI.

4.2 Inversion of Complex Near-Surface Using Data with Free Surface-Related Multiples

As shown by the authors earlier [15], taking the surface-related (SR) multiples into account during the inversion reduces the resolution and the information content of the FWI results. However, it increases their stability in the presence of uncorrelated noise. Therefore, at the first stage of FWI, we use the entire wavefield, including SR multiples. The results of the near-surface inversion are shown in Fig. 7. The inversion was performed using the temporal frequencies range from 3 10 Hz, and the target area was limited up to the depths of 1 km. As one can see, with such an acquisition system and frequency range of the source signal (presence of low frequencies), we successfully identified high-speed anomalies. However, areas directly under the traps were restored with significant distortion. Therefore, in subsequent stages of FWI (see Sect. 4.3), to improve the restored model's quality, it is proposed to use the data without SR multiples.

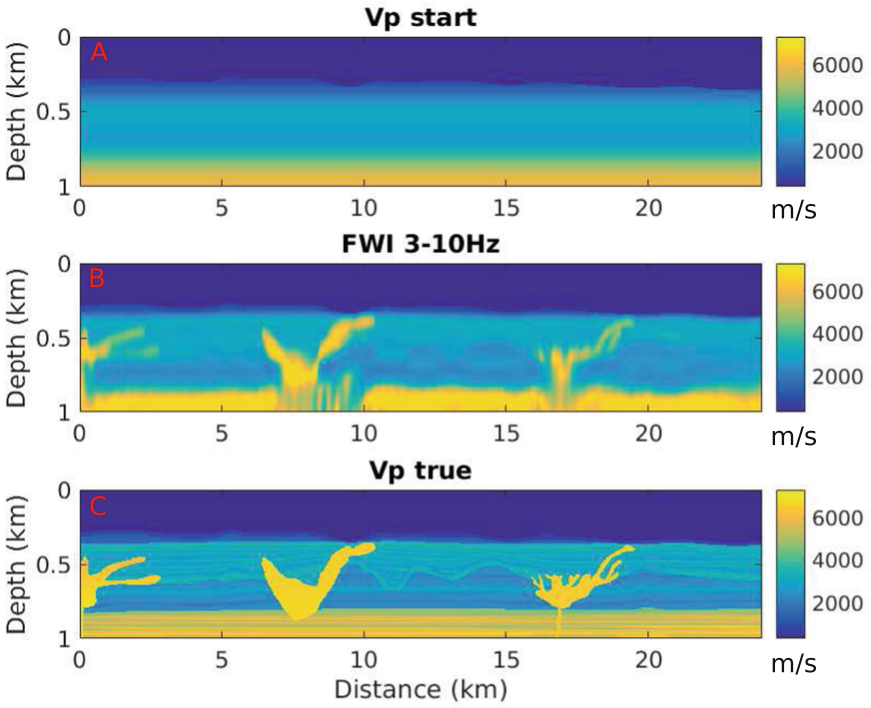

Fig. 7. The inversion of complex near surface results: starting model (a), FWI results (b), and the true model (c).

The Influence of Maximum Offset in the Data on the Near-Surface Inversion

To analyze the maximum source-receiver offsets' influence on the inversion results, we consider three different FWI scenarios. We used the same source geometry and the same receiver steps but varied the maximum offset. In the first case, we used 3 km maximum offset, in the second - 5 km (previous results), and in the last - 7 km. Typically for the real acquisition in Eastern Siberia, 5 km is the maximum available offset, and the most common maximum source-receiver offset is 3 km. The near-surface FWI results for a different scenarios are presented in Fig. 8. As one may observe, for the reasonable offset ranges (from 3 km to 7 km), there are no significant differences in the inversion results, which means that the maximum offset in the data does not affect the near-surface FWI results in our case.

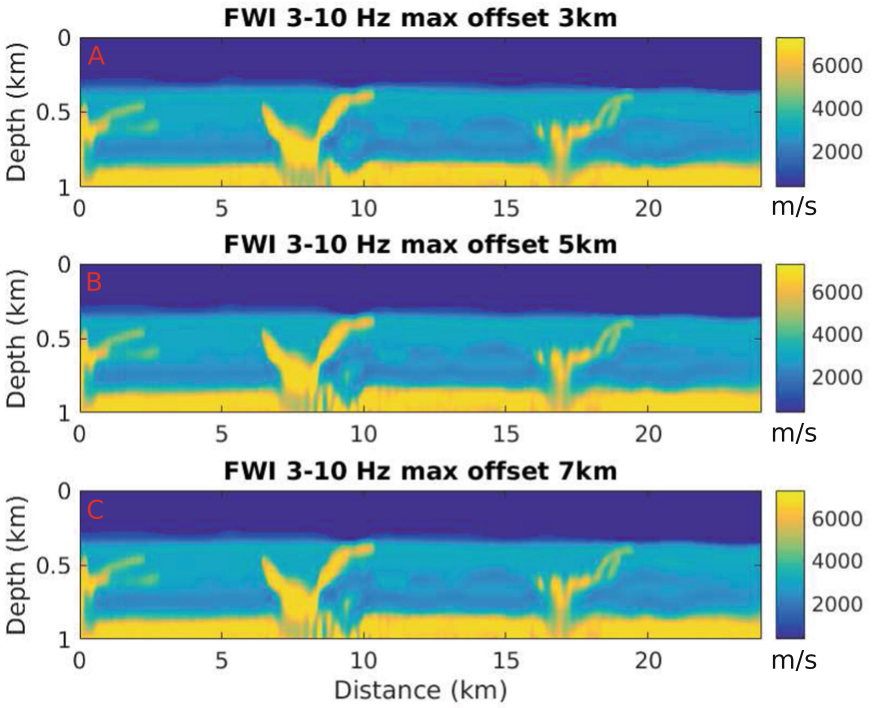

Fig. 8. The influence of the maximum offset on the inversion results: FWI using offsets up to the 3 km (a), 5 km (b), and 7 km (c).

The Influence of the Lower Available Time Frequency in the Data on the Near-Surface Inversion

As we have seen, the influence of the maximum offset on inversion results is negligible within a reasonable range. Now we are interested in the influence of the lower available temporal frequency in the observed data. We performed three FWI tests with a lower frequency 3 Hz, 5 Hz 7 Hz. The inversion results are shown in Fig. 9. We see that lower frequency affects the near-surface FWI results substantially. The bigger the lower frequency, the worse trap intrusions reconstruction we observe. The comparative analysis of relative error between the reconstructed near-surface model and true model is presented in Fig. 10. Furthermore, as we increase the lower temporal frequency, we decrease the data fitting. The corresponding misfit functional behaviour during FWI iterations for different scenarios plotted in logarithmic scale is shown in Fig. 11.

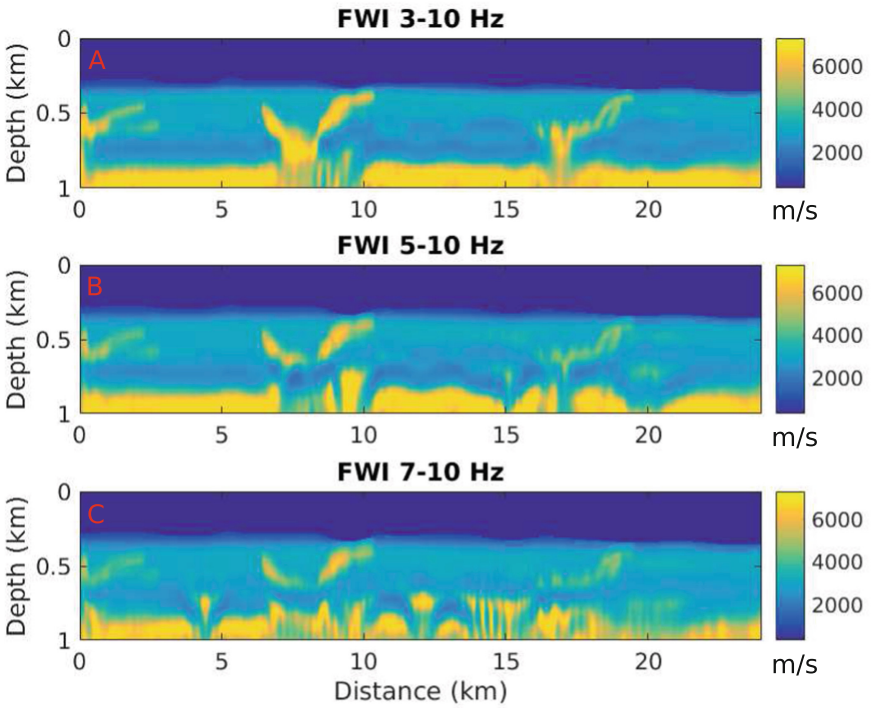

Fig. 9. The influence of the lower available time frequency in the data on the inversion results: FWI using lower 3 Hz (a), 5 Hz (b), 7 Hz (c).

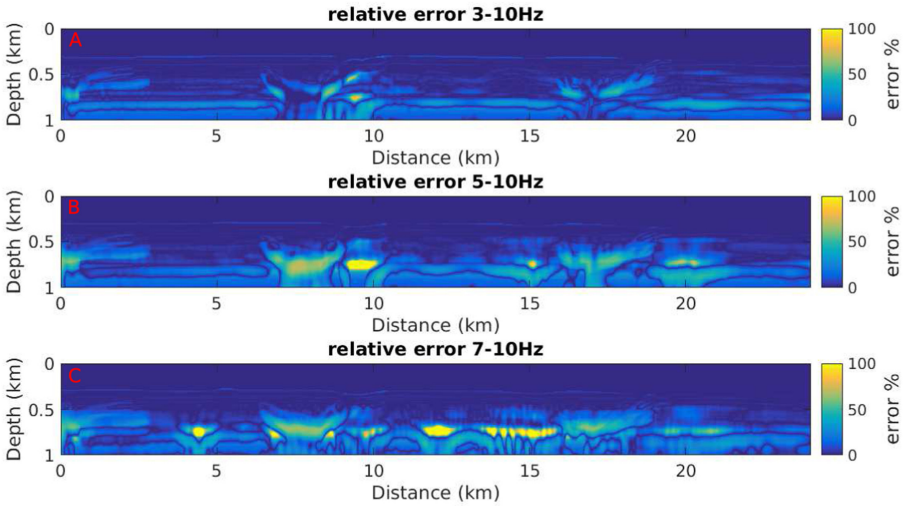

Fig. 10. The relative error between true near-surface model and the FWI model using lower 3 Hz (a), 5 Hz (b), 7 Hz (c).

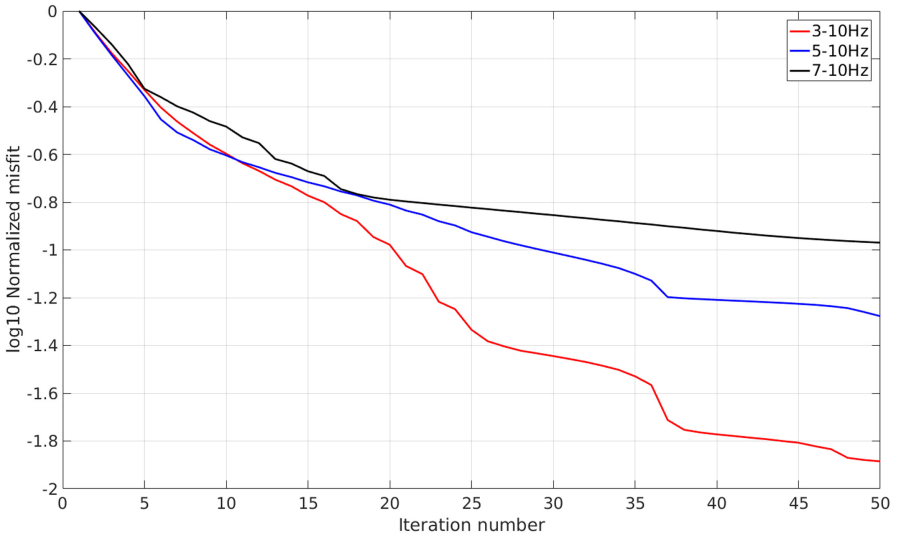

Fig. 11. The L_2 mistfits between observed and modelled data during inversion for FWI scenario using lower 3 Hz (red plot), 5 Hz (blue plot), 7 Hz (black plot). (Color figure online)

4.3 Inversion of Deep Target Horizons Using Data Without Free Surface-Related Multiples

For reconstruction of the deep target horizons to improve the restored model's quality, it is proposed to use the data without multiples associated with the

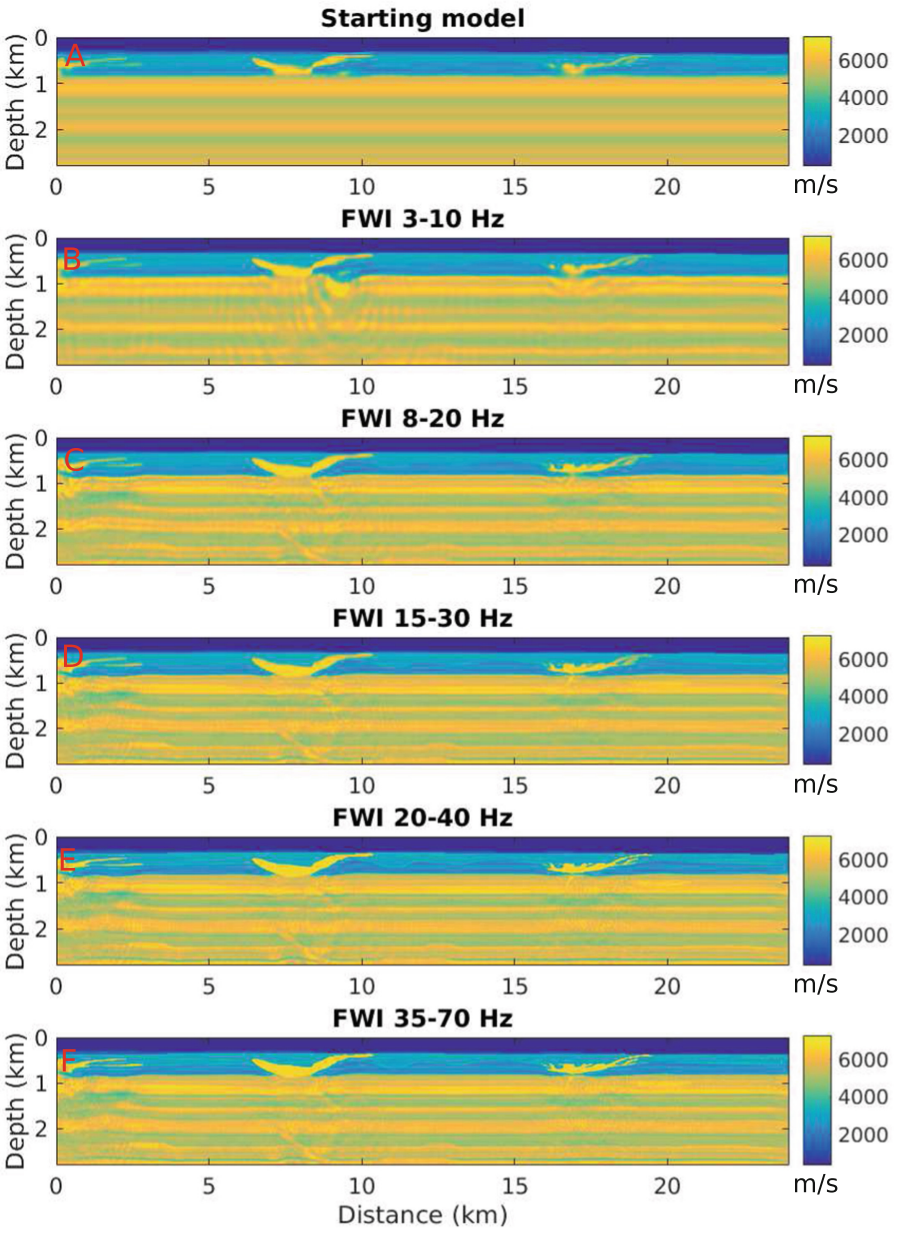

Fig. 12. The inversion results using the data without free surface related multiples for different frequencies ranges: starting model (a), FWI 3–10 Hz (b), FWI 8–20 Hz (c), FWI 15–30 Hz (d), FWI 20–40 Hz (e), and FWI 35–70 Hz (f).

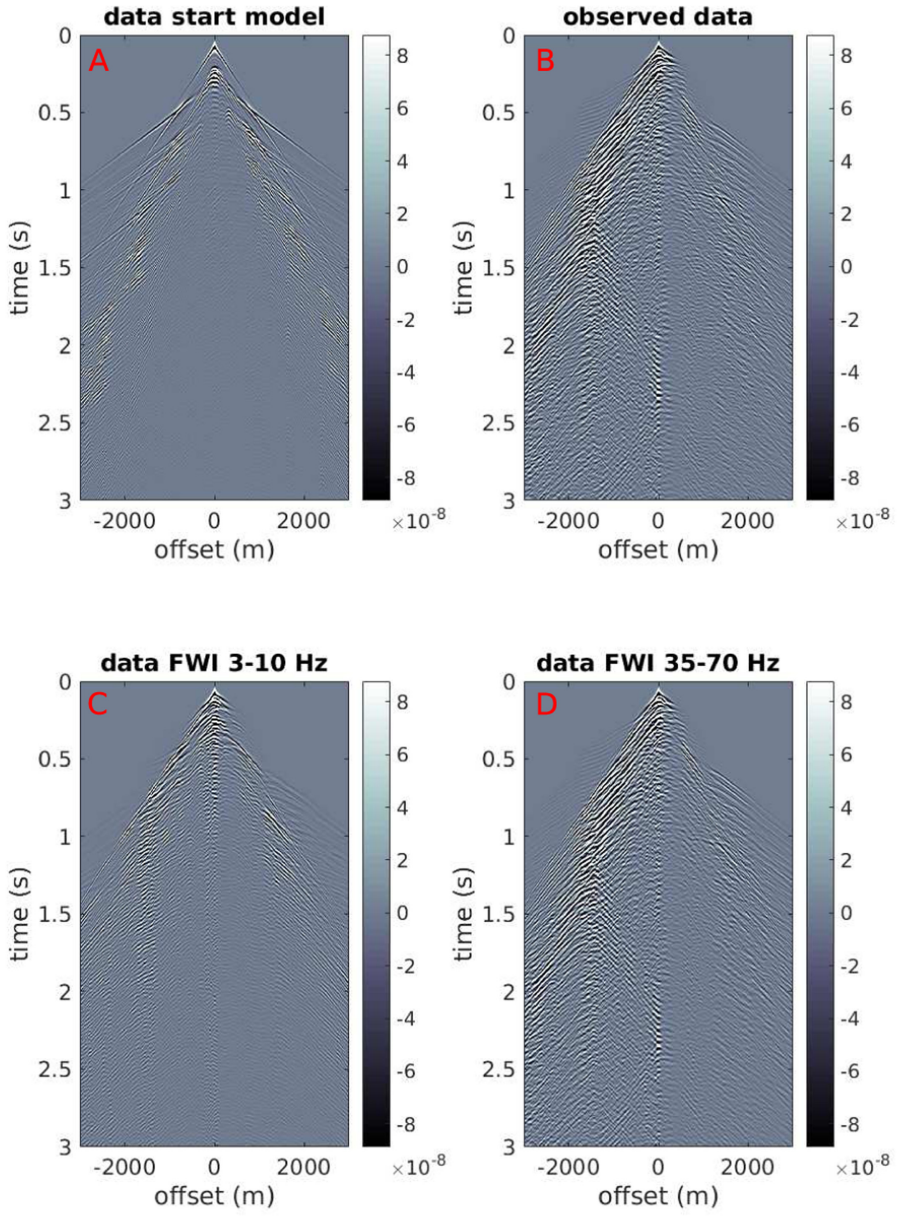

Fig. 13. The data comparison for shot located at x = 8 km on a different inversion stages: data in starting model before the near-surface FWI (a), the data modelled in a true model (b), the data after near-surface FWI (c), and the data in the final FWI model (d).

presence of a free surface. While performing FWI in the time-frequency domain, it is common practice to use overlapping frequency groups. In our case, after the near-surface reconstruction in the frequency range [3, 10] Hz with SR multiples, we used the following set of frequency groups to be used in FWI without SR multiples: [3, 10] Hz, [8, 20] Hz, [15, 30] Hz, [20, 40] Hz and [35, 70] Hz. The starting velocity model for each frequency group is the velocities from the previous FWI run (e.g. the output of FWI for a frequency range [3, 10] Hz is an input for [8, 20] Hz FWI, and so on). The evolution of depth velocity model reconstruction for a different frequency group is shown in Fig. 12. As one can see, we managed to get a detailed depth velocity model restoration in almost the entire region. To demonstrate the data fitting, we calculate the seismogram for a shot located at x = 8 km (see Fig. 13). As one may observe, the starting model's synthetics does not explain the observed data, while the final FWI model interprets most of the observed data.

5 Conclusions

The paper considers an approach to the near-surface P-velocity distribution inversion based on the FWI. As the authors showed earlier, the attraction of multiples associated with a free surface reduces the resolution of this approach. However, it increases the stability of the solution in the presence of uncorrelated noise. Therefore, at the first stage of FWI, one uses the entire wavefield, including free surface-related multiples. Further, the data after multiples suppression is used. The results obtained demonstrate the FWI method's ability to reconstruct complex geological structures of the near-surface area, even in the presence of high-velocity anomalies (trap intrusions).

Acknowledgements. K. Gadylshin is supported by RSF grant 21-71-20002, he performed all numerical FWI experiments. The numerical results of the work were obtained using computational resources of Peter the Great Saint-Petersburg Polytechnic University Supercomputing Center (scc.spbstu.ru).

References

1. Bloor, R., Whaler, K.: The generation of near-surface-layer models from seismic reflection traveltimes. Geophys. J. Int. **119**(3), 693–705 (1994)
2. Dou, S., et al.: Distributed acoustic sensing for seismic monitoring of the near surface: a traffic-noise interferometry case study. Sci. Rep. **7**, 11620 (2017)
3. Liu, F., Morton, S.A., Ma, X., Checkles, S.: Some key factors for the successful application of full-waveform inversion. Lead. Edge **32**(9), 1124–1129 (2013)
4. Silvestrov, I., Neklyudov, D., Kostov, C., Tcheverda, V.: Full-waveform inversion for macro velocity model reconstruction in look-ahead offset vertical seismic profile: numerical singular value decomposition-based analysis. Geophys. Prospect. **61**(6), 1099–1113 (2013)
5. Tanis, M.C., et al.: Diving-wave refraction tomography and reflection tomography for velocity model building. In: SEG 76th Annual International Meeting, Expanded Abstracts, pp. 3340–3344 (2006)

6. Tcheverda, V., Gadylshin, K.: Elastic full-waveform inversion using migration-based depth reflector representation in the data domain. Geosciences **11**, 76 (2021)
7. Tverdokhlebov, D.N., Korobkin, V.S., Danko, E.A., Kashirina, E.G., Filichev, A.V., Gaiduk, A.V.: Model based multiple waves suppression based on modeling algorithm. Geofizika **1**, 2–14 (2018)
8. Xie, H., et al.: Imaging complex geology through challenging surface terrain - a case study from West China. First Break **33**(3), 55–69 (2015)
9. Li, L.M., Luo, S.X.: The tomographic inversion static correction on complex three-dimensional surface model. Oil Geophys. Prospect. **38**(6), 636–641 (2003)
10. Zhang, W., Zhang, J.: Full waveform tomography with consideration for large topography variations. In: SEG Annual Meeting Expanded Abstracts, San Antonio, pp. 2539–2542 (2011)
11. Socco, L.V., et al.: Geophysical investigation of the Sandalp rock avalanche deposits. J. Appl. Geophys. **70**, 277–291 (2010)
12. Piatti, C., Socco, L.V., Boiero, D., Foti, S.: Constrained 1D joint inversion of seismic surface waves and P-refraction traveltimes. Geophys. Prospect. **61**, 77–93 (2013)
13. Shen, X., Tonellot, T., Luo, Y.: A new waveform inversion workflow: application to near-surface velocity estimation in Saudi Arabia. In: SEG Annual Meeting expanded abstracts, Las Vegas, USA (2012)
14. Bretaudeau, F., Brossier, R., Leparoux, D.: 2D elastic full waveform imaging of the near-surface: application to synthetic and physical modeling data sets. Near Surface Geophys. **11**(3), 307–316 (2013)
15. Gadylshin, K., Bakulin, A., Dmitriev, M., Golikov, P., Neklyudov, D., Tcheverda, V.: Effect of free-surface related multiples on near surface velocity reconstruction with acoustic frequency domain FWI. In: 76th European Association of Geoscientists and Engineers Conference and Exhibition 2014: Experience the Energy - Incorporating SPE EUROPEC 2014, Amsterdam, Netherlands, 16–19 June 2014, pp. 357–361 (2014)